

One-dimensional turbulence (ODT): computationally efficient modeling and simulation of turbulent flows

Victoria B. Stephens, David O. Lignell*

Chemical Engineering Department, Brigham Young University, Provo, UT 84602, USA

Abstract

One-dimensional turbulence (ODT) is an accurate and computationally efficient technique for modeling turbulent flows. ODT has been applied to a wide range of flow problems including reaction, multiphase, differential diffusion, heat release, buoyancy, and wall flows. Applications include use as a standalone model and as a closure for large-eddy simulation (LES). Its strength lies in the ability to capture a full range of turbulent length and time scales. The ODT model is strongly coupled with its implementation, complicating its formulations. We present a modern, open-source, object-oriented C++ implementation of ODT. This code can be used as a starting point to understand, apply, and extend the ODT model, enabling its further application to turbulent flow research.

Keywords: turbulence, reacting flows, one-dimensional turbulence

*Corresponding author.

Email address: davidlignell@byu.edu (David O. Lignell)

Code Metadata

Nr.	Code metadata description	Please fill in this column
C1	Current code version	1.0
C2	Permanent link to code/repository used for this code version	https://github.com/BYUignite/ODT
C3	Code Ocean compute capsule	N/A
C4	Legal Code License	MIT
C5	Code versioning system used	Git
C6	Software code languages, tools, and services used	C++, Python 3.x, YAML,
C7	Compilation requirements, operating environments & dependencies	CMake 3.12+, Cantera, Git, Doxygen (optional)
C8	If available Link to developer documentation/manual	ODT style guide
C9	Support email for questions	davidlignell@byu.edu

Table 1: Code metadata (mandatory)

1. Motivation and significance

Turbulent flows characterize the vast majority of fluid flows in practical engineering applications, and simulations of turbulent flows provide researchers with valuable insights into complex systems, particularly reacting turbulent flows such as combustion processes. Turbulence is a complex phenomenon that affects the full range of a flow's length and time scales. As a result, resolving the entire flow field by numerically solving the Navier-Stokes equations of fluid flow, as is done in direct numerical simulations (DNS), requires substantial computational resources. DNS is a powerful research tool, but its high computational cost makes it intractable for simulating most practical engineering flows. In order to achieve numerical solutions to practical flow problems, researchers use alternative frameworks that model turbulence rather than resolving it directly.

Large-eddy simulations (LES) address the problem of wide-ranging length and time scales by combining direct resolution of grid-scale quantities, as in DNS, with subgrid modeling of smaller turbulence structures. The more complex the flow, the more modeling is required; for example, a jet flame simulation might require subgrid modeling for the combustion chemistry, radiative heat transfer, and soot chemistry in addition to turbulence structures, all of which form a tightly coupled system in which each model interacts heavily with the others. While subgrid modeling makes LES more computationally

22 affordable than DNS, it can introduce empiricism into simulations, which
23 can lead to inaccurate results. Additionally, unresolved quantities are often
24 parameterized in state space with empirical relationships or assumed distri-
25 butions that lack universal applicability. LES is a valuable simulation tool,
26 but its approach to turbulence modeling can introduce unwanted empiricism
27 and make errors difficult to isolate and quantify.

28 The one-dimensional turbulence model (ODT) functionally reverses the
29 LES approach, modeling large-scale turbulent advection and directly resolv-
30 ing small-scale flow structures, simulating the full range of length and time
31 scales in a single dimension. Depending on the configuration, large-scale
32 structures can be easier to model than small-scale structures, especially in
33 reacting flows. ODT’s direct resolution of fine scales in one dimension by-
34 passes subgrid modeling issues that complicate LES. Previous studies show
35 that ODT can attain accuracy comparable to DNS at a fraction of the com-
36 putational cost [1, 2], making it an attractive tool for simulating turbulent
37 flows. Because the ODT model is one-dimensional, it is limited to homoge-
38 neous or boundary-layer flows, such as jets, wakes, and mixing layers, but
39 these types of flows are common in nature and central to turbulence research.
40 ODT’s computational efficiency and resolution of a full range of scales make it
41 a valuable tool that complements experimental studies and other simulation
42 tools like DNS and LES.

43 Early applications of ODT focused on homogeneous turbulence, wakes,
44 and mixing layers [3, 4, 5]. Later extension to variable-density flows and
45 a spatial downstream coordinate system facilitated its growth and appli-
46 cation to more complex flows, including combustion in jet flames [6, 7, 8,
47 9, 10, 11, 12, 13], counterflow flames [14], wall fires [15], and sooting flames
48 [1, 16, 17, 18, 19], as well as other particle flows [20, 21, 22, 23]. ODT has also
49 served to complement LES through subgrid modeling studies [24, 25, 26] and
50 has been applied to various other flow configurations such as double-diffusive
51 interfaces [27], Rayleigh-Taylor mixing [28], and stratified turbulence [29].
52 Most recently, the ODT code was extended to include cylindrical and spher-
53 ical coordinate systems [30, 31, 32].

54 During the recent implementation of the cylindrical and spherical model
55 formulations, the ODT code was drastically overhauled and reorganized, re-
56 sulting in its current configuration. The ODT code presented here is a pared
57 down version of the development code, representing the fundamental aspects
58 of the ODT model and its most reliable functions. The example case in
59 Section 3 is a representative sample of the ODT code’s capabilities as it is
60 presented here. Future releases will expand this code’s functionality with
61 additional features currently in development.

62 2. Software description

63 2.1. Model description

64 The ODT model is described in detail in the literature [3, 5, 33, 30, 34];
 65 only a brief explanation will be given here. In ODT, turbulent advection is
 66 modeled with stochastic processes called eddy events, which punctuate the
 67 solution of unsteady, one-dimensional transport equations for mass, momen-
 68 tum, and enthalpy. The ODT code uses a Lagrangian finite-volume formula-
 69 tion for diffusive advancement in which mass stays constant within each grid
 70 cell while cell volumes increase or decrease according to cell dilation via an
 71 adaptive mesh refinement [34].

72 Transport equations for mass, momentum, and enthalpy in the tempo-
 73 ral formulation of ODT take the following generic form, derived from the
 74 Reynolds Transport Theorem [35] for a given scalar quantity per unit mass
 75 β :

$$\frac{d\beta}{dt} = -\frac{j_{\beta,e}A_{x,e} - j_{\beta,w}A_{x,w}}{\rho V} + \frac{S_{\beta}}{\rho V}. \quad (1)$$

76 The first and second terms on the right-hand-side of this equation are the
 77 diffusive transport and source terms, respectively. Here, the term *diffusive* is
 78 not specific to mass transfer, but may refer to the transport of, e.g., heat,
 79 mass, and momentum, depending on the identity of the scalar β . In practice,
 80 we refer to the transport term as the “mixing term”. The symbols shown in
 81 Equation 1 are defined as follows: j_{β} is the diffusion flux of scalar β across
 82 the cell face area A_x , where the subscripts e and w refer to the “east” and
 83 “west” faces of a given grid cell, respectively; S_{β} is the Lagrangian source
 84 term derived from the conservation law for β ; ρ represents mass density; and
 85 V represents cell volume. The generic transport equation differs slightly in
 86 the spatial formulation of ODT, but its form is similar, so we omit it here for
 87 brevity. The system of ordinary differential equations (ODEs) that results
 88 is well behaved at all grid points and in all geometries in their finite-volume
 89 forms. For details on transport equation derivation and use in both the
 90 temporal and spatial formulations of ODT, see [30].

91 Eddy events occur as a Poisson process in accordance with their eddy
 92 rates, where a given eddy event of size l and location x_0 has an eddy timescale
 93 t and an associated eddy rate $1/t$. Three user-defined ODT parameters
 94 control the eddy event process: the eddy rate parameter C scales the rate of
 95 occurrence of the eddies; the viscous penalty parameter Z suppresses small
 96 eddies; and the large eddy suppression parameter β_{LES} constrains eddies to
 97 those with timescales proportional to the elapsed simulation time. Sampled
 98 eddies that do not fit the defined parameters are rejected and not applied to
 99 the domain.

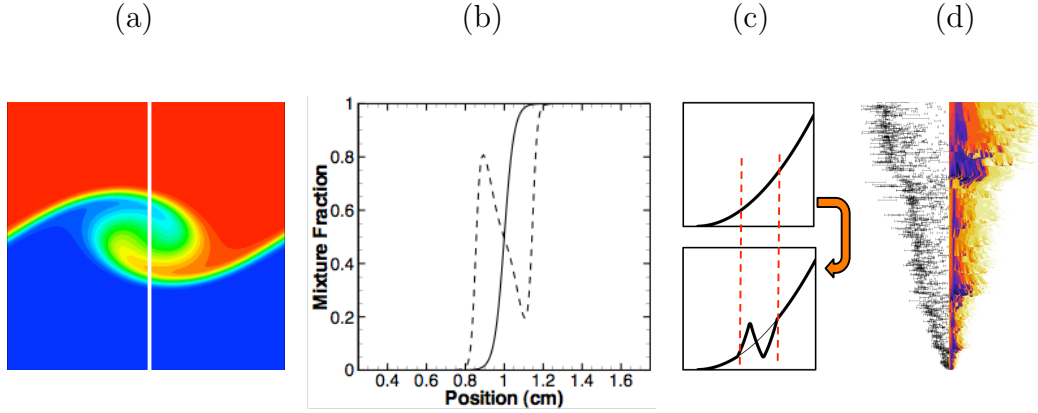


Figure 1: Schematic diagram of a triplet map. From left to right: (a) simulation of a single “eddy”, a two-dimensional Kelvin-Helmholtz instability with a vertical white line-of-sight; (b) mixture fraction profile along the indicated line-of-sight before and after the eddy showing increased gradients and surface area; (c) a triplet map operates on a profile to produce a mapped profile with three copies, compressed and lined up, with the middle copy spatially inverted; (d) illustrative eddy event sizes and locations with corresponding temperature profile for a single ODT realization of a wall fire, adapted from [15].

100 Eddy events modify domain variables using “triplet maps”, as illustrated
 101 in Figure 1. In an eddy region of size l , transported property profiles are
 102 modified (mapped) by making three copies, compressing each spatially by a
 103 factor of three, and realigning them with the middle copy spatially reversed.
 104 This map is continuous, conserves all quantities and statistical moments, in-
 105 creases scalar gradients, and decreases length scales consistent with turbulent
 106 eddies in real flows. Subsequent eddies in the same region will result in a
 107 cascade of scales. The eddy rates, used to sample and select eddy events,
 108 depend on eddy size and the local kinetic energy consistent with turbulent
 109 scaling laws.

110 Eddy events occur concurrently with diffusive advancement via solution
 111 of the system of unsteady one-dimensional transport equations. In this way,
 112 the ODT code marches in time or space until it reaches the simulation end
 113 point. Due to the stochastic nature of eddy events, each ODT simulation,
 114 or realization, is different, even when it is provided with the same input
 115 parameters. In order to obtain statistically stable data for a given set of
 116 parameters, we run many realizations with the same input parameters and
 117 then gather statistics over these realizations. This is done via post-processing
 118 tools. Post-processing is specific to a given case and the needs of the user.
 119 Examples of post-processing files are included for different cases provided
 120 with the ODT code, as discussed further in Section 2.3.4.

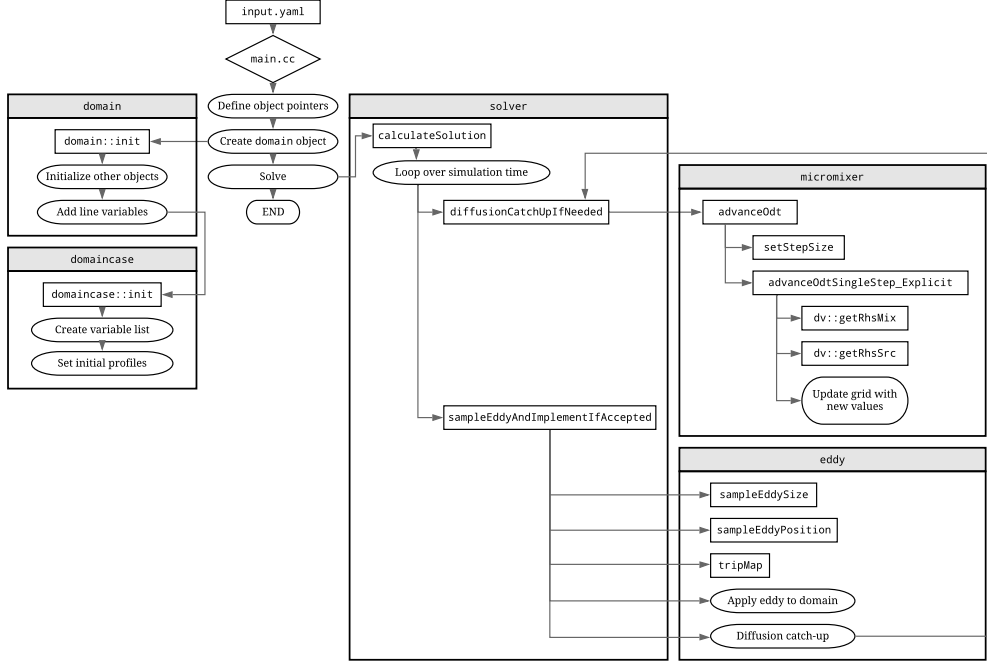


Figure 2: Structural outline of the ODT code, including its major class objects. For brevity, this diagram makes two simplifications. First, it assumes that diffusive advancement in the `micromixer` uses an explicit solution method; in practice, users specify either an explicit, semi-implicit, or Strang split method. Second, it implies that all of the eddy events sampled by the `eddy` object are applied to the domain; in reality, eddy events are filtered through several rejection tests (omitted from this figure for clarity) before acceptance and application to the domain.

121 2.2. Software Architecture

122 The ODT package consists primarily of an object-oriented C++ code re-
 123 sponsible for running flow simulation cases and generating data. The package
 124 also contains auxiliary data processing and visualization tools, written mostly
 125 in Python. The post-processing tools are case-specific but will be addressed
 126 generally in Section 2.3.

127 Figure 2 illustrates the ODT code’s most important objects and structural
 128 features. User inputs are provided to the executable in YAML [36] format via
 129 `input.yaml`; the location of the specific `input.yaml` file to be used is deter-
 130 mined by the case name and case type specified in the run script. The `main`
 131 function defines storage for the main objects, but, once created, the `domain`
 132 object is responsible for object initialization as well as variable initialization
 133 and storage via a case-specific `domaincase` object.

Three primary objects handle the code’s main functions: the **solver**, **micromixer**, and **eddy** objects. The **solver** coordinates the ODT solution process, marching along the simulation time and invoking diffusive advancement and eddy events. The **micromixer** handles diffusive advancement by setting step sizes, interacting with the transported domain variables, and solving the system of ODEs defined by Equation 1 (or its equivalent in the spatial formulation). The **micromixer** includes three solution methods that can be specified in **input.yaml**: a first-order explicit Euler method (pictured in Figure 2), a first-order semi-implicit method, and a second order Strang splitting method [37]. The latter two methods are useful for treating stiff chemistry, with source terms integrated using CVODE [38]. In reacting flow cases, enthalpy and chemical species mass fractions are transported, and physical properties and kinetic rates are computed with Cantera [39]. The **micromixer** is also the code’s primary point of interaction with the **mesher** object (not pictured in Figure 2), which manages the adaptive grid functions. Finally, the **eddy** object manages eddy event selection and implementation, which proceeds as described in Section 2.1.

2.3. Workflow

This section outlines the process a user goes through in order to successfully build the ODT code and run a simulation. ODT is a standalone, self-contained package, and users interact with its files primarily via the command line rather than a graphical interface. For more details, please see the package documentation.

Within the main download package, several directories organize the ODT code. The **source**, **build**, and **run** directories contain the ODT source code, compilation tools, and run scripts, respectively. The **input** directory contains subdirectories corresponding to several possible case types, each populated with the appropriate input files. The **data** directory, initially empty, holds the raw data files and runtime information generated by ODT, as well as post-processed data files generated from within the **post** directory. Finally, the **docs** directory contains documentation optionally generated by Doxygen [40] during the build process.

2.3.1. Building ODT

The ODT build process is automated with CMake. The user navigates to the **build** directory and edits the CMake configuration file. The CMake configuration file specifies Cantera’s location and must be changed to reflect the local installation location. For reacting flows, the chemical reaction rates can be computed by Cantera (default), or a from a user-specified function,

172 specified at compile time. Once the configuration settings are updated, the
173 user runs CMake to apply the changes.

174 The `yaml-cpp` package is required in order to process input files. If it
175 has not yet been installed, it must be built and installed at this point. For
176 convenience, the ODT package automates this process. YAML need only be
177 installed once for a given instance of the ODT package. Rebuilding the ODT
178 code with CMake does not affect the YAML installation.

179 Once CMake and YAML have been prepared, the user can build the
180 ODT code with the `make` command, which places the code executable in the
181 `run` directory. The most common errors that occur during the build process
182 involve incorrect file paths or incomplete installation of required packages.
183 See the build documentation for troubleshooting help.

184 Once the code is built, the user may optionally build a local copy of the
185 documentation via Doxygen, which must be previously installed. This step is
186 not required in order to run the ODT code. As an alternative, documentation
187 can be accessed at the code repository wiki.

188 2.3.2. *Input files*

189 User-modified input files are located within the `input` directory, which
190 contains subdirectories that correspond to various case types that can be run
191 with ODT. At minimum, a case's subdirectory must contain an `input.yaml`
192 file, but may contain other files, or subfolders with supplementary informa-
193 tion.

194 The `input` directory also contains the `gas_mechanisms` subdirectory, which
195 contains chemical mechanism files that can be used in reacting flow cases.
196 For cases in which a chemical mechanism is not required, the `not_used.xml`
197 mechanism file is specified in `input.yaml`. Note that the chemical mech-
198 anism chosen for the case and specified in the input file must match the
199 mechanism specified in the CMake configuration file during the ODT build
200 process.

201 Input files contain simulation parameters in a human-readable format
202 parsed by YAML. Within `input.yaml`, parameters are organized into sec-
203 tions, several of which are common to all input files. Parameter values present
204 in the provided input files may be considered defaults that can be used to
205 run a successful simulation of that case type. General code parameters are
206 stored in the `params` class. Variables needed in a simulation but not provided
207 in an input file (not recommended), are either given defaults specified in the
208 `params` class or result in an error message. Details about individual param-
209 eters, including usage and typical values, are covered in the documentation.

210 2.3.3. Running ODT

211 To run a simulation, users must then navigate to the **run** directory, which
212 contains the **odt.x** executable and several possible run scripts. The simplest
213 option is **runOneRlz.sh**, which runs one realization of ODT in the specified
214 configuration. In this run script, the user must alter two variables near the
215 top of the file: **inputDir**, which specifies which input directory and files to
216 use; and **caseName**, which provides a name for the simulation and the data
217 files it outputs. The **runManyRlz.sh** script runs many realizations in serial,
218 one after the other; it differs from **runOneRlz.sh** only in that the user must
219 also alter the **nRlz** variable, which specifies the number of realizations to
220 run. Each realization has a different seed value, which can be randomized
221 or directly specified in the input file. To run the simulation with either
222 **runOneRlz.sh** or **runManyRlz.sh**, save the run script and execute it at the
223 command line. Users will see some output on the command line, but no data,
224 which is instead output to the **data** directory.

225 ODT simulations can also be run in parallel using MPI. Two run scripts,
226 **slrmJob.sh** and **slrmJob_array.sh**, are configured using Slurm [41], a com-
227 mon workload manager used for massively parallel computing resources. This
228 allows many ODT realizations to run in parallel rather than in serial, reduc-
229 ing overall simulation time. Individual realizations are independent (embar-
230 rassingly parallel), but users must take care with case names and input file
231 changes to ensure that individual realizations or entire cases are not overrid-
232 den accidentally.

233 2.3.4. Data files and post-processing

234 For a given simulation, data is output to the **data** directory, which con-
235 tains subdirectories for each simulation, specified by the **caseName** variable
236 in the run script. Figure 3 illustrates the structure of the **data** directory and
237 the locations of files within it. Each case folder is subdivided into **input**,
238 **runtime**, **data**, and **post**. The **input** folder contains a copy of the input
239 files used for the simulation; **runtime** contains runtime output, including
240 eddy event information; **data** contains the raw data files; and **post** contains
241 post-processed data files once they are generated.

242 To use post-processing tools, users navigate to the **post** directory. Within
243 the **post** directory, data processing tools are organized by case type, which
244 is specified in **input.yaml** and determines case-specific variables and simu-
245 lation setup parameters (refer to the **domaincase** object in Figure 2). Each
246 set of post-processing tools is different, but may contain some combination of
247 **Jupyter notebooks**, Python scripts (often coordinated by a **driver.py** file),
248 experimental data files for comparison and plot generation, or other supple-
249 mentary files. Post-processed data and generated plots are deposited in the

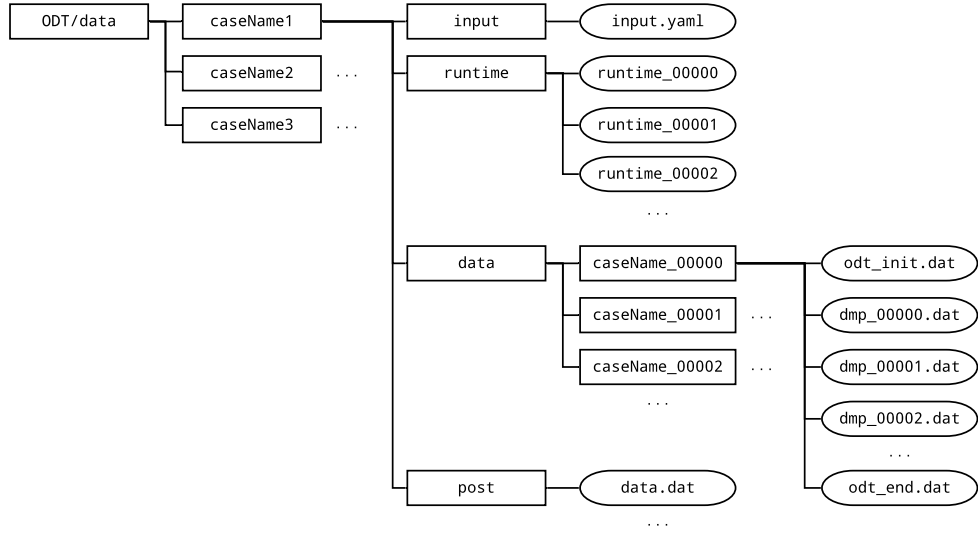


Figure 3: Data folder structure and file locations. Boxes indicate folders and ovals indicate files. For a given simulation, **caseName** will be replaced with the case name specified in the run script. The number attached to **caseName** folder names and to **runtime** data files indicates the realization number. The number attached to **dmp** files indicates the **index of the list of “dump” times included in, or generated from the information in input.yaml.**

250 data directory, within the appropriate caseName/post folder.

251 As part of the post-processing tools, there is a post/tools directory that
252 contains two files: data_py.py and data_tools.py. The first of these can be
253 used to convert the text data files generated during a run into binary numpy
254 files. This can reduce both the number of data files and the file sizes. The
255 number of files is reduced since all code realizations at a given output time
256 are saved in the same binary file. The data_tools.py file is a module that
257 contains a number of functions for processing the data files, such as functions
258 to

- 259 • get the data from a given realization,
- 260 • return the number of realizations,
- 261 • get a list of the variable names in the data files,
- 262 • compute axial locations in the spatial ODT formulation,
- 263 • query a parameter from the input file,
- 264 • return the stoichiometric mixture fraction for combustion/mixing prob-
265 lems, and
- 266 • compute the domain bounds.

267 In addition, a few functions are provided for doing interpolation/extrapolation,
268 and computing probability density functions (PDFs), and weighted PDFs.
269 Many of these functions take an argument that is a dictionary of case-specific
270 information, such as the case name and paths for key directories. This dictio-
271 nary is set in the post-processing driver script based only on the user-specified
272 case name.

273 3. Example Case: Canonical Jet Flame

274 ODT is uniquely suited to reacting flow simulations. Here, we present
275 illustrative ODT simulation results of a round, turbulent jet flame based on
276 and compared to the experimental DLR-A flame of Meier et al. [42]. This
277 canonical flame configuration has been used extensively to study and validate
278 turbulent combustion models [43, 44, 45, 46, 47, 48].

279 The DLR-A fuel stream is mixture of 22.1% CH₄, 33.2% H₂, and 44.7%
280 N₂ (by volume) that issues into dry air via a nozzle with an inner diameter
281 of 8 mm at a mean exit velocity of 42.2 m·s⁻¹. The coflow air stream issues
282 from a concentric nozzle 140 mm in diameter at a velocity of 0.3 m·s⁻¹. The
283 reported jet Reynolds number is 15,200.

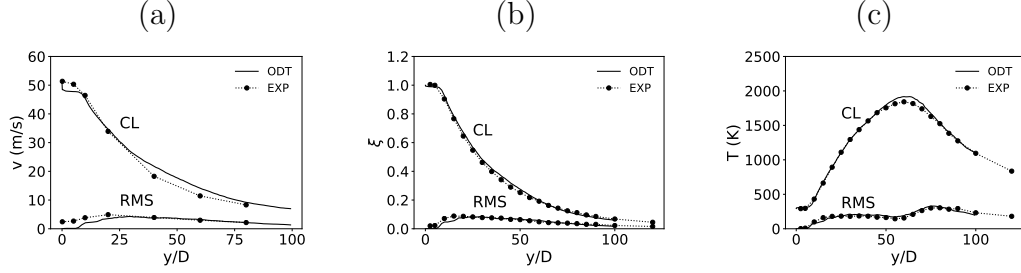
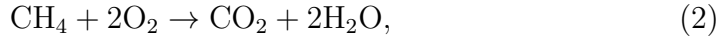


Figure 4: DLR jet flame example case results: (a) mean axial velocity and RMS velocity along the centerline versus downstream location; (b) mean axial mixture fraction and RMS mixture fraction along the centerline versus downstream location; (c) mean axial temperature (K) and RMS temperature (K) along the centerline versus downstream location.

Previous ODT studies of turbulent jet flames have used the temporal planar formulation, but the spatial cylindrical formulation developed recently [30] more closely matches the experimental configuration. This simulation uses the experimentally reported velocity profiles and jet dimensions. The fuel was diluted with N_2 in the experimental flame to minimize radiative heat losses, and radiation is ignored in the simulation. This flame has a low Reynolds number, and the combustion chemistry proceeds quickly. The ODT simulation transports the chemical species O_2 , N_2 , CH_4 , H_2 , H_2O , and CO_2 . We assume that reactions proceed to the products of complete combustion and apply simple, fast reaction rates according to the following chemical equations:



These assumptions are reasonable for illustrating ODT in the DLR-A reacting jet configuration with variable properties and heat release.

This simulation uses ODT parameters $C = 20$, $\beta_{LES} = 17$, and $Z = 400$. The values of C and β_{LES} were adjusted to give good agreement with the experimental data, and the value of Z is the same as the spatial simulations in [15]. 1024 independent flow realizations were performed in parallel and the results ensemble averaged. Downstream distance y and radial position r are normalized by the jet diameter D .

Figure 4 displays the simulation results: axial mean and centerline values for (a) axial velocity v , (b) mixture fraction ξ , and (c) temperature T . The ODT results track the experimental data well for all three variables. The centerline temperature peaks about 100 K above the experimental data, but

296 this small difference can be attributed to thermal radiation (which was ne-
297 glected in this simulation) and the assumption that reactions proceed to the
298 products of complete combustion rather than their equilibrium state. The
299 centerline velocity shows a fast initial decrease that can be attributed to dif-
300 fusion. Similarly, the increase in centerline velocity RMS values is delayed;
301 this occurs due to the elapsed time model for large eddy suppression, which
302 limits disturbances in the early stages of the flow to small eddies that occur
303 on the jet edges away from the centerline.

304 To replicate this example case, build the code with the `CHEMISTRY =`
305 `SIMPLEDLR` flag in the `user_config` file and edit the desired run script with
306 `inputDir = "../input/jetFlame/DLR_A"` and a new case name such as
307 `caseName = "jetFlame_example"`. The input file for this case, located at
308 `ODT/input/jetFlame/DLR_A/input.yaml`, contains the appropriate param-
309 eters and does not need to be modified to match this example case. See the
310 code documentation for data post-processing instructions.

311 4. Impact

312 The ODT model is complex, challenging to implement, and difficult to
313 cleanly separate from its implementation, all of which presents barriers to
314 practitioners who wish to use the model. For instance, triplet maps can be
315 represented mathematically but are usually implemented as previously de-
316 scribed, assuming an adaptive grid with variable cell sizes. Alternative for-
317 mulations are used for fixed grids. The code presented here reduces these bar-
318 riers by providing an open-source, well-documented, modularly styled code
319 that can be used directly or modified to suit particular research goals. Its
320 structure facilitates addressing new research questions, such as soot-flame-
321 radiation-chemistry interactions, multi-phase reacting flows using Lagrangian
322 particle models (such as diesel sprays), and coupled near-wall heat and mo-
323 mentum transfer. The code presented here has been extended to and demon-
324 strated in such systems already, facilitated by the object-oriented structure.
325 For example, this code has been extended to solve steady laminar flamelets
326 [49], requiring inheritance from the `solver`, `micromixer`, and `dv` (domain
327 variable) classes.

328 The structure of the ODT code, using an adaptive mesh and a Lagrangian
329 formulation for diffusive advancement of transport equations, has several
330 advantages, including simplicity of formulation and computational efficiency.
331 The adaptive mesh minimizes the number of computational cells required and
332 can be adapted to any variable of interest. This is especially important for
333 flows with complex and expensive chemistry and flows with widely varying
334 resolution demands such as near-wall flows. The Lagrangian formulation

implies that cell faces move with fluid velocity (such as is present during flame expansion, for example). This treatment is inherently stable, removing the need for complex and diffusive hyperbolic conservation law treatments and their associated CFL constraints. The conservation equations, as in Equation 1, are similarly simplified.

The code has been run on Linux, Mac, and Windows machines, including parallel clusters of up to 512 processor cores. Several research groups have used the code and contributed to its development. These include groups at Sandia National Laboratories, Brandenburg University of Technology Cottbus-Senftenberg, Chalmers University, and Combustion Science and Engineering, Inc. The latter company is the only organization known to use the code in a commercial setting, though on a combustion research project.

5. Conclusion

A clean and extensible implementation of the one-dimensional turbulence (ODT) model has been presented in an open-source, object-oriented C++ framework, motivated by advanced turbulent reacting flow research. The build process, directory structure, input file format, run process, and post-processing procedure were described in detail, including a representative reacting jet example case. Access to a proven, documented code and a modern build procedure will aid researchers in applying and extending the model to new research questions.

6. Conflict of Interest

There are no known conflicts of interest associated with this publication and there has been no significant financial support for this work that could have influenced its outcome.

Acknowledgements

Special thanks to Alan R. Kerstein for his significant contributions to model development. Additional thanks to Heiko Schmidt, Juan Medina, and Marten Klein of Brandenburg University of Technology Cottbus-Senftenberg, Michael Oevermann and Marco Fistler of Chalmers University of Technology, and John Hewson of Sandia National Laboratories for code contributions, and insightful conversations.

368 References

- 369 [1] D. O. Lignell, G. C. Fredline, A. D. Lewis, Comparison of one-
370 dimensional turbulence and direct numerical simulations of soot for-
371 mation and transport in a nonpremixed ethylene jet flame 35 (2) (2015)
372 1199–1206. doi:10.1016/j.proci.2014.05.046.
- 373 [2] A. W. Abboud, C. Schulz, T. Saad, S. T. Smith, D. D. Harris, D. O.
374 Lignell, A numerical comparison of precipitating turbulent flows between
375 large-eddy simulation and one-dimensional turbulence 61 (10) (2015)
376 3185–3197. doi:10.1002/aic.14870.
- 377 [3] A. R. Kerstein, One-dimensional turbulence: model formulation and ap-
378 plication to homogeneous turbulence, shear flows, and buoyant stratified
379 flows 392 (1999) 277–334. doi:10.1017/S0022112099005376.
- 380 [4] A. R. Kerstein, T. D. Dreeben, Prediction of turbulent free shear flow
381 statistics using a simple stochastic model 12 (2) (2000) 418–424. doi:
382 10.1063/1.870319.
- 383 [5] A. R. Kerstein, W. T. Ashurst, S. Wunsch, V. Nilsen, One-dimensional
384 turbulence: vector formulation and application to free shear flows 447
385 (2001) 85–109. doi:10.1017/S0022112001005778.
- 386 [6] T. Echekki, A. R. Kerstein, T. D. Dreeben, J.-Y. Chen, ‘one-dimensional
387 turbulence’ simulation of turbulent jet diffusion flames: model formu-
388 lation and illustrative applications 125 (3) (2001) 1083–1105. doi:
389 10.1016/S0010-2180(01)00228-0.
- 390 [7] J. C. Hewson, A. R. Kerstein, Stochastic simulation of transport and
391 chemical kinetics in turbulent CH₄/H₂/N₂ flames 5 (4) (2001) 669–697.
392 doi:10.1088/1364-7830/5/4/309.
- 393 [8] J. C. Hewson, A. R. Kerstein, Local extinction and reignition in non-
394 premixed turbulent CH₄/H₂/N₂ jet flames 174 (5-6) (2002) 35–66.
395 doi:10.1080/713713031.
- 396 [9] D. O. Lignell, D. S. Rappleye, One-dimensional-turbulence simulation
397 of flame extinction and reignition in planar ethylene jet flames 159 (9)
398 (2012) 2930–2943. doi:10.1016/j.combustflame.2012.03.018.
- 399 [10] N. Punati, J. C. Sutherland, A. R. Kerstein, E. R. Hawkes, J. H. Chen,
400 An evaluation of the one-dimensional turbulence model: comparison
401 with direct numerical simulations of CO/H₂ jets with extinction and

- 402 reignition 33 (1) (2011) 1515–1522. doi:10.1016/j.proci.2010.06.
403 127.
- 404 [11] A. Abdelsamie, D. O. Lignell, D. Thévenin, Comparison between ODT
405 and DNS for ignition occurrence in turbulent premixed jet combustion:
406 safety-relevant applications 231 (10) (2017) 1709–1735. doi:10.1515/
407 zpch-2016-0902.
- 408 [12] D. O. Lignell, V. B. Lansinger, A. R. Kerstein, A cylindrical formula-
409 tion of the one-dimensional turbulence (ODT) model for turbulent jet
410 flames, in: AIChE Annual Meeting 2017, American Institute of Chemi-
411 cal Engineers, 2017.
- 412 [13] B. Goshayeshi, J. C. Sutherland, Prediction of oxy-coal flame stand-off
413 using high-fidelity thermochemical models and the one-dimensional tur-
414 bulence model 35 (3) (2015) 2829–2837. doi:10.1016/j.proci.2014.
415 07.003.
- 416 [14] Z. Jozefik, A. R. Kerstein, H. Schmidt, S. Lyra, H. Kolla, J. H. Chen,
417 One-dimensional turbulence modeling of a turbulent counterflow flame
418 with comparison to DNS 162 (8) (2015) 2999–3015. doi:10.1016/j.
419 combustflame.2015.05.010.
- 420 [15] E. I. Monson, D. O. Lignell, M. A. Finney, C. Werner, Z. Jozefik,
421 A. R. Kerstein, R. S. Hintze, Simulation of ethylene wall fires using
422 the spatially-evolving one-dimensional turbulence model 52 (1) (2016)
423 167–196. doi:10.1007/s10694-014-0441-2.
- 424 [16] J. C. Hewson, A. J. Ricks, S. R. Tieszen, A. R. Kerstein, R. O. Fox,
425 Conditional-moment closure with differential diffusion for soot evolution
426 in fire, in: Center for Turbulence Research, Proceedings of the Summer
427 Program 2006, Stanford University, 2006.
- 428 [17] J. C. Hewson, A. J. Ricks, S. R. Tieszen, A. R. Kerstein, R. O. Fox, On
429 the transport of soot relative to a flame: modeling differential diffusion
430 for soot evolution in fire, in: H. Bockhorn, A. D’Anna, A. F. Sarofim,
431 H. Wang (Eds.), Combustion Generated Fine Carbonaceous Particles,
432 KIT Scientific Publishing, 2009, pp. 571–588.
- 433 [18] D. O. Lignell, J. C. Hewson, One-dimensional turbulence simulation:
434 overview and application to soot formation in nonpremixed flames, in:
435 SIAM Conference on Computational Science and Engineering, 2015.

- 436 [19] A. J. Ricks, J. C. Hewson, A. R. Kerstein, J. P. Gore, S. R.
437 Tieszen, W. T. Ashurst, A spatially developing one-dimensional tur-
438 bulence (ODT) study of soot and enthalpy evolution in meter-scale
439 buoyant turbulent flames 182 (1) (2010) 60–101. doi:10.1080/
440 00102200903297003.
- 441 [20] G. Sun, J. C. Hewson, D. O. Lignell, Evaluation of stochastic particle
442 dispersion modeling in turbulent round jets 89 (2017) 108–122. doi:
443 10.1016/j.ijmultiphaseflow.2016.10.005.
- 444 [21] J. R. Schmidt, J. O. L. Wendt, A. R. Kerstein, Non-equilibrium wall
445 deposition of inertial particles in turbulent flow 137 (2) (2009) 233–257.
446 doi:10.1007/s10955-009-9844-8.
- 447 [22] G. Sun, D. O. Lignell, J. C. Hewson, C. R. Gin, Particle dispersion
448 in homogeneous turbulence using the one-dimensional turbulence model
449 26 (10) (2014) 103301. doi:10.1063/1.4896555.
- 450 [23] M. Fistler, D. O. Lignell, A. R. Kerstein, M. Oevermann, Numerical
451 studies of turbulent particle-laden jets using spatial approach of one-
452 dimensional turbulence, in: ILASS-Europe 28th Conference on Liquid
453 Atomization and Spray Systems, 2017.
- 454 [24] S. Cao, T. Echekki, A low-dimensional stochastic closure model for com-
455 bustion large-eddy simulation 9. doi:10.1080/14685240701790714.
- 456 [25] R. C. Schmidt, A. R. Kerstein, S. Wunsch, V. Nilsen, Near-wall LES
457 closure based on one-dimensional turbulence modeling 186 (1) (2003)
458 317–355. doi:10.1016/S0021-9991(03)00071-8.
- 459 [26] R. C. Schmidt, A. R. Kerstein, R. McDermott, ODTLES: A multi-
460 scale model for 3D turbulent flow based on one-dimensional turbulence
461 modeling 199 (13-16) (2010) 865–880. doi:10.1016/j.cma.2008.05.
462 028.
- 463 [27] E. Gonzalez-Juez, A. R. Kerstein, D. O. Lignell, Fluxes across double-
464 diffusive interfaces: a one-dimensional-turbulence study 677 (2011) 218–
465 254. doi:10.1017/jfm.2011.78.
- 466 [28] E. Gonzalez-Juez, A. R. Kerstein, D. O. Lignell, Reactive Rayleigh-
467 Taylor turbulent mixing: a one-dimensional-turbulence study 107 (5)
468 (2013) 506–525. doi:10.1080/03091929.2012.736504.

- [29] S. Wunsch, A. R. Kerstein, A model for layer formation in stably stratified turbulence 13 (3) (2001) 702–712. doi:10.1063/1.1344182.
- [30] D. O. Lignell, V. B. Lansinger, J. Medina, M. Klein, A. R. Kerstein, H. Schmidt, M. Fistler, M. Oevermann, One-dimensional turbulence modeling for cylindrical and spherical flows: model formulation and application 32 (4) (2018) 495–520. doi:10.1007/s00162-018-0465-1.
- [31] M. Klein, D. O. Lignell, H. Schmidt, Map-based modeling of turbulent convection: application of the one-dimensional turbulence model to planar and spherical geometries, in: International Conference on Rayleigh-Benard Turbulence, 2018.
- [32] M. Klein, D. O. Lignell, H. Schmidt, Stochastic modeling of temperature and velocity statistics in spherical-shell convection, in: EGU Conference on Recent developments in Geophysical Fluid Dynamics, 2019.
- [33] W. T. Ashurst, A. R. Kerstein, One-dimensional turbulence: variable-density formulation and application to mixing layers 17 (2). doi:10.1063/1.1847413.
- [34] D. O. Lignell, A. R. Kerstein, G. Sun, E. I. Monson, Mesh adaption for efficient multiscale implementation of one-dimensional turbulence 27 (3-4) (2013) 273–295. doi:10.1007/s00162-012-0267-9.
- [35] Y. A. Çengel, J. M. Cimbala, Fluid Mechanics, 2nd Edition, Çengel series in engineering thermal-fluid sciences, McGraw-Hill Higher Education, 2010.
- [36] J. Beder, yaml-cpp v0.6.3 (2008).
URL <https://github.com/jbeder/yaml-cpp/>
- [37] G. Strang, On the construction and comparison of difference schemes 5 (3) (1968) 506–517. doi:10.1137/0705041.
- [38] A. C. Hindmarsh, R. Serban, D. R. Reynolds, CVODE, https://computing.llnl.gov/sites/default/files/public/cv_guide.pdf (2020).
URL <https://computing.llnl.gov/projects/sundials/cvode>
- [39] D. G. Goodwin, R. L. Speth, H. K. Moffat, B. W. Weber, Cantera (2018). doi:10.5281/zenodo.1174508.
URL <https://cantera.org/>

- [40] D. van Heesch, Doxygen (2018).
URL <https://www.doxygen.nl/>
- [41] A. B. Yoo, M. A. Jette, M. Grondona, Slurm: simple linux utility for resource management, in: D. G. Feitelson, L. Rudolph, U. Schwiegelshohn (Eds.), Job Scheduling Strategies For Parallel Processing, Vol. 2862 of Lecture notes in computer science, 0302-9743, Springer, 2003, pp. 44–60. doi:10.1007/10968987-3.
- [42] W. Meier, R. S. Barlow, Y.-L. Chen, J.-Y. Chen, Raman/Rayleigh/LIF measurements in a turbulent CH₄/H₂/N₂ jet diffusion flame: experimental techniques and turbulence–chemistry interaction 123 (3) (2000) 326–343. doi:10.1016/S0010-2180(00)00171-1.
URL <https://tnfworkshop.org/data-archives/simplejet/dlrflames/>
- [43] H. Pitsch, Unsteady flamelet modeling of differential diffusion in turbulent jet diffusion flames 123 (3) (2000) 358–374. doi:10.1016/S0010-2180(00)00135-8.
- [44] R. P. Lindstedt, H. Ozarovskiy, Joint scalar transported PDF modeling of nonpiloted turbulent diffusion flames 143 (4) (2005) 471–490. doi:10.1016/j.combustflame.2005.08.030.
- [45] H. Wang, S. B. Pope, Large eddy simulation/probability density function modeling of a turbulent CH₄/H₂/N₂ jet flame 33 (1) (2011) 1319–1330. doi:10.1016/j.proci.2010.08.004.
- [46] M. Fairweather, R. M. Woolley, First-order conditional moment closure modeling of turbulent, nonpremixed methane flames 138 (1-2) (2004) 3–19. doi:10.1016/j.combustflame.2004.03.001.
- [47] K. W. Lee, D. H. Choi, Prediction of NO in turbulent diffusion flames using eulerian particle flamelet model 12 (5) (2008) 905–927. doi:10.1080/13647830802094351.
- [48] K. W. Lee, D. H. Choi, Analysis of NO formation in high temperature diluted air combustion in a coaxial jet flame using an unsteady flamelet model 52 (5-6) (2009) 1412–1420. doi:10.1016/j.ijheatmasstransfer.2008.08.015.
- [49] N. Peters, Laminar diffusion flamelet models in non-premixed turbulent combustion, Progress in Energy and Combustion Science 10 (1984) 319–339. doi:10.1016/0360-1285(84)90114-X.

537 **Current executable software version**

538 Software information is provided in Table 2.

Nr.	(Executable) software meta-data description	Please fill in this column
S1	Current software version	1.0
S2	Permanent link to executables of this version	For example: https://github.com/BYUignite/ODT
S3	Legal Software License	MIT
S4	Computing platforms/Operating Systems	Linux, OS X, Microsoft Windows
S5	Installation requirements & dependencies	CMake 3.12+, Cantera, Git, Doxygen (optional)
S6	If available, link to user manual - if formally published include a reference to the publication in the reference list	https://github.com/BYUignite/ODT
S7	Support email for questions	davidlignell@byu.edu

Table 2: Software metadata (optional)